

Synergistic Deep Graph Clustering Network

Benyu Wu[✉], Shifei Ding[✉], *Senior Member, IEEE*, Xiao Xu[✉], Lili Guo[✉], *Member, IEEE*, Ling Ding[✉],
and Xindong Wu[✉], *Fellow, IEEE*

Abstract—Employing graph neural networks (GNNs) to learn cohesive and discriminative node representations for clustering has shown promising results in deep graph clustering. However, existing methods disregard the reciprocal relationship between representation learning and structure augmentation. This study suggests that enhancing embedding and structure synergistically becomes imperative for GNNs to unleash their potential in deep graph clustering. A reliable structure promotes obtaining more cohesive node representations, while high-quality node representations can guide the augmentation of the structure, enhancing structural reliability in return. Moreover, the generalization ability of existing GNNs-based models is relatively poor. While they perform well on graphs with high homogeneity, they perform poorly on graphs with low homogeneity. To this end, we propose a graph clustering framework named **Synergistic Deep Graph Clustering Network (SynC)**. In our approach, we design a **Transform Input Graph Auto-Encoder (TIGAE)** to obtain high-quality embeddings for guiding structure augmentation. Then, we re-capture neighborhood representations on the augmented graph to obtain clustering-friendly embeddings and conduct self-supervised clustering. Notably, representation learning and structure augmentation share weights, significantly reducing the number of model parameters. Additionally, we introduce a **structure fine-tuning strategy** to improve the model’s generalization. Extensive experiments on benchmark datasets demonstrate the superiority and effectiveness of our method. The code is released at [GitHub](#)¹ and [Code Ocean](#)².

Index Terms—Deep graph clustering, graph auto-encoder, self-supervised learning, graph refinement

I. INTRODUCTION

WITH the rapid advancement of graph neural networks (GNNs), employing GNNs to learn structural information has garnered significant attention and has yielded notable results in deep graph clustering (DGC) [1]–[6]. One of the most representative graph neural networks is the graph convolutional network (GCN) [7], including its advanced version, the graph auto-encoder (GAE) [8], which learns low-dimensional representations of the input. GAE encounters the representation collapse issue that nodes from different

This work was supported by the National Natural Science Foundation of China under Grants No.62276265 and No.61976216 (*Corresponding author: Shifei Ding*).

Benyu Wu, Shifei Ding, Xiao Xu, and Lili Guo are with the School of Computer Science and Technology, China University of Mining and Technology, Xuzhou, 221116, China and also with the Mine Digitization Engineering Research Center of Ministry of Education, Xuzhou, 221116 China (e-mail: {bywu; dingsf; xu_xiao; liligu}@cumt.edu.cn).

Ling Ding is with the College of Intelligence and Computing, Tianjin University, Tianjin, 300350 China (e-mail: dltjdx2022@tju.edu.cn).

Xindong Wu is with the Key Laboratory of Knowledge Engineering with Big Data (the Ministry of Education of China), Hefei University of Technology, 230009 China (e-mail: xwu@hfut.edu.cn).

¹<https://github.com/Marigoldwu/SynC>

²<https://codeocean.com/capsule/8085961/tree>

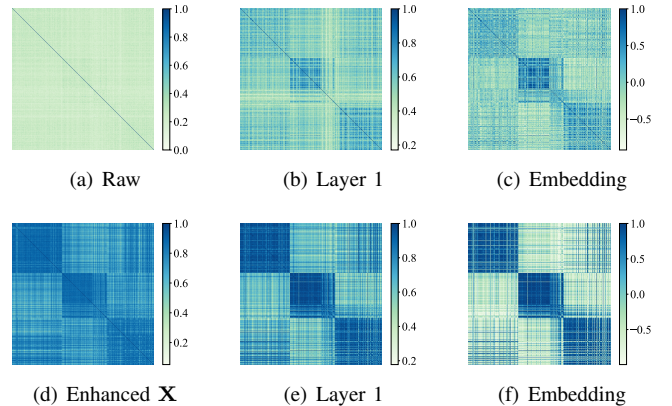


Fig. 1. Comparison of nodes similarity on the dataset ACM. The first row represents GAE, and the second represents GAE with linear transformation applied to X .

categories are mapped to similar representations [9]. Fig. 1(a)–1(c) illustrate the cosine similarity matrices among nodes on the ACM. It is evident that even after the transformation by GAE, the nodes from the three categories still cannot be well distinguished, which validates the phenomenon observed by Liu et al. Nevertheless, as illustrated in Fig. 1(d)–1(f), the final embeddings exhibit a significant improvement in discriminability after performing a linear transformation with bias on the original feature. Based on this exciting observation, we infer that the quality of the input attributes plays a crucial role in determining the discriminability of the GAE embeddings.

Moreover, with a deeper understanding of the message propagation mechanism of GCN, we can consider the over-smoothing effect [10] as a potential benefit for clustering, particularly when it facilitates intra-cluster smoothing. Zhao et al. [11] have also highlighted that the representations of any nodes within the same class are identical after applying multi-layer GCNs on an ideal graph or a class-homophilic graph. Therefore, GCN-based models typically do not perform well on graphs with low homogeneity, which is a manifestation of poor generalization. Graph Augmentation Learning (GAL) is a technique that can improve the generalization of graph models and has been widely studied. Using neural networks to predict graph structures [11] is a bold attempt. However, this method often employs inconsistent networks between predicting the graph and downstream tasks, leading to complex optimization for model. Additionally, non-differentiable sampling techniques are required between the two, hindering gradient backpropagation, and typically necessitating the use of Gumbel-Softmax reparameterization trick [12] to circumvent this issue. However, graph structure and downstream tasks

are often closely related. For instance, in graph clustering, high homogeneity graphs are more conducive to learning more cohesive node representations. In such cases, using two separate networks overlooks the reciprocal relationship between representation learning and structure augmentation. If weights are shared between representation learning and structure augmentation, this issue can be resolved. On one hand, sharing weights allows these two components to learn consistent representations synergistically. On the other hand, optimizing only one component reduces the model size and eliminates the need for Gumbel-Softmax reparameterization.

By integrating all the insights above and addressing the challenges encountered in deep clustering with GNNs, we propose a novel graph clustering framework called Synergistic Deep Graph Clustering Network (SynC). Specifically, we address the issue of representation collapse in the GAE by introducing the Transform Input Graph Auto-Encoder (TIGAE). Using a linear transformation with bias before GAE, TIGAE indirectly incorporates explicit structural information to optimize the feature and improve the embeddings' intra-cluster similarity and inter-cluster discriminability. We predict the existence probability of edges between nodes via using high-quality embeddings obtained by TIGAE. Then, we employ a structure fine-tuning strategy that considers multiple factors (e.g. pruning, link, weighting) to effectively refine the predicted graph so that the refined graph can benefit the attributes aggregation through the TIGAE, which is vital for improving generalization. The augmented graph is fed into another TIGAE to obtain improved embeddings. These two TIGAEs share weights. Combining structure augmentation with representation enhancement in this mutual boost manner, we refer to it as a synergistic architecture of representation learning and structure augmentation. Finally, we conduct clustering via self-supervised learning. The main contributions of this paper are summarized as follows.

- We have developed a graph clustering framework called SynC, which stands for Synergistic Deep Graph Clustering Network. This framework utilizes the high-quality embeddings learned by the TIGAE to enhance both representation and structure synergistically, thereby improving intra-cluster similarity and inter-cluster discriminability.
- We have developed a new GAE architecture, specifically for deep graph clustering, called Transform Input Graph Auto-Encoder (TIGAE). This architecture optimizes the input for graph convolution to enhance attributes by indirectly incorporating explicit structural information, effectively alleviating the representation collapse of GAE.
- We have employed a structure fine-tuning strategy that considers multiple factors to enhance generalization.
- Extensive experiments demonstrate the outstanding performance of our proposed method. SynC also achieves state-of-the-art results in graph clustering tasks.

The rest of the paper is organized as follows. Section II introduces the most related work about DGC and GAL, respectively. Section III details our proposed SynC. Section IV analyzes the extensive experimental results. Finally, we make a conclusion and outlook in Section V.

II. RELATED WORK

A. Deep Graph Clustering

Deep graph clustering is dedicated to dividing nodes into distinct clusters by learning node embeddings, ensuring higher similarity within the same cluster than between different clusters. In the earlier methods, they solely learned representations by mapping attributes to lower-dimensional embeddings. Subsequently, clustering was performed using techniques like K-Means [13] or self-supervised methods, such as DEC [14] and IDEC [15].

Graph representation learning has advanced significantly since the proposal of GCN, driving research on DGC. Techniques such as GAE and GAT [16] have been employed to improve performance by learning more cohesive embeddings. Various variants of GAE have been proposed, such as ARGAE [17], MGAE [18], R-GAE [19], MaskGAE [20], and GraphMAE2 [21]. However, SDCN [22] emphasizes the importance of simultaneously learning structure and attribute information to enrich embeddings. SDCN lacks a dynamic fusion mechanism and reliable self-supervised target distribution. DFCN [23] improves performance through a dynamic cross-modal fusion mechanism and a triple self-supervised learning strategy to address the limitations. CaEGCN [24] introduces cross-attention fusion mechanism to integrate representation learned by auto-encoder and GAE. Moreover, AGC and IAGC [25] employ an adaptive graph convolution method to exploit high-order graph structure for DGC.

While cohesion is crucial for clustering, discriminability is also an essential factor influencing clustering performance. DCRN [9] improves the discriminability of embeddings by reducing information correlation at the dual level. AGC-DRR [3] reduces information redundancy in input and latent feature spaces to distinguish samples effectively. R²FGC [26] captures intrinsic relational and semantic information among non-independent and differently distributed nodes to reduce redundancy and obtain discriminative embeddings. Although these advanced methods demonstrated strong clustering performance, they have become increasingly complex. Additionally, breakthroughs have been made in graph clustering based on contrastive learning, with more refined methods for selecting positive and negative samples, including hard ones [5], [27]–[29], and so are the methods based on multi-view clustering [30]–[32]. Research progress has also been made in clustering large-scale graph data [33] and unknown cluster number data [34]. Although significant progress has been made in deep graph clustering research, there are still substantial challenges in improving the quality of graph data, enhancing the embeddings' discriminability, and elevating the stability and scalability of the model. Research on deep graph clustering is extensive. For more methods, please refer to the review paper by Liu et al. [35], as well as their shared papers and codes at Awesome-Deep-Graph-Clustering.

B. Graph Augmentation Learning

Graph Augmentation Learning (GAL) is a crucial technique for improving graph representation learning and enhancing model robustness, especially when dealing with incomplete or

noisy data [36]. Two representative methods for micro-level augmentation are DropGNN [37] and DropEdge [38]. To improve the performance of GNNs, DropGNN randomly removes nodes from graph, while DropEdge randomly removes edges. However, it is essential to note that excessive or indiscriminate pruning can restrict potential performance gains.

Additionally, latent connections in the graph can be utilized to achieve better performance. GAUG [11] employs neural networks to perform edge prediction, followed by applying the predicted graph in downstream tasks. GACN [39] leverages the cosine similarity between node embeddings and then adds the most similar nodes to each node in the original graph. PASTEL [40] combines position encoding with node features to learn a graph with improved intra-class connectivity. It utilizes class-wise conflict metrics as edge weights to guide the learning process. DFCN-RSP [41] introduces a random walk mechanism to filter out noisy edges and enhance reliable edges by measuring the local structural similarity between nodes. While these methods effectively augment the graph, they either rely on simplistic knowledge to guide the augmentation or involve complex modules.

This paper proposes utilizing the representation learning network for structure augmentation, achieving a synergistic interaction between representation and structure. A structure fine-tuning strategy is also employed to obtain a well-structured graph. Our approach benefits the mutual boost of representation learning and structure augmentation, facilitating the learning of clustering-friendly embeddings.

III. METHODOLOGY

The framework diagram of SynC is illustrated in Fig. 2. In this section, we will elaborate on the following key topics:

- T1. How does TIGAE effectively alleviate the representation collapse issue of GAE?
- T2. What factors should be considered when fine-tuning the predicted graph?
- T3. How does SynC achieve synergistic interaction of representation learning and structure augmentation for learning clustering-friendly embeddings?
- T4. How to build the end-to-end clustering framework?
- T5. What is the computational complexity of SynC?

A. Notation Definition

Given an undirected graph \mathcal{G} with \mathcal{E} edges and N nodes belonging to k categories. The connectivity of the graph is represented by the adjacency matrix $\mathbf{A} \in \mathbb{R}^{N \times N}$. We define $\tilde{\mathbf{A}} = \mathbf{A} + \mathbf{I}$ as the adjacency matrix with self-loop, where \mathbf{I} is the identity matrix. The symmetrically normalized adjacency matrix is denoted as $\tilde{\mathbf{L}} = \tilde{\mathbf{D}}^{-\frac{1}{2}} \tilde{\mathbf{A}} \tilde{\mathbf{D}}^{-\frac{1}{2}}$, where $\tilde{\mathbf{D}} = \text{diag}(\sum_{j=1}^N \tilde{\mathbf{A}}_{1j}, \sum_{j=1}^N \tilde{\mathbf{A}}_{2j}, \dots, \sum_{j=1}^N \tilde{\mathbf{A}}_{Nj})$ is the degree matrix. Node attributes are represented by the matrix $\mathbf{X} \in \mathbb{R}^{N \times d}$, which can be linearly transformed to \mathbf{X}_t or \mathbf{X}_p , where d represents the dimension of attributes and t, p are used to differentiate between different stages of the linearly transformed \mathbf{X} . The cosine similarity between node features is $\mathcal{S}(\mathbf{X}) = \frac{\mathbf{x}}{\|\mathbf{x}\|_2} \times \frac{\mathbf{x}^\top}{\|\mathbf{x}^\top\|_2}$. We need to optimize our model iteratively, so we use the symbol l in the upper right corner to

TABLE I
NOTATIONS SUMMARY.

Notations	Explanations
$\mathbf{I} \in \mathbb{R}^{N \times N}$	Identity matrix
$\mathbf{X} \in \mathbb{R}^{N \times d}$	Attribute matrix
$\mathbf{X}_t, \mathbf{X}_p \in \mathbb{R}^{N \times c}$	Transformed \mathbf{X} in different phases
$\mathbf{A}, \mathbf{A}_p \in \mathbb{R}^{N \times N}$	Original and augmented adjacency matrix
$\tilde{\mathbf{A}} \in \mathbb{R}^{N \times N}$	Adjacency matrix with self-loop
$\mathbf{A}_s \in \mathbb{R}^{N \times N}$	Adjacency matrix sampled by Bernoulli
$\hat{\mathbf{A}} \in \mathbb{R}^{N \times N}$	Reconstructed graph in the first phase
$\hat{\mathbf{A}}_p \in \mathbb{R}^{N \times N}$	Edge probability predicted in the second phase
$\tilde{\mathbf{L}} \in \mathbb{R}^{N \times N}$	Symmetric normalized adjacency matrix of $\tilde{\mathbf{A}}$
$\tilde{\mathbf{D}} \in \mathbb{R}^{N \times N}$	Degree matrix of $\tilde{\mathbf{A}}$
$\mathbf{M}, \mathbf{M}_e \in \mathbb{R}^{N \times N}$	Weighted matrix of \mathbf{A}_s
$\mathbf{W}_i \in \mathbb{R}^{d_i \times d_{i+1}}$	Parameters matrices
$\mathbf{H}, \mathbf{Z} \in \mathbb{R}^{N \times m}$	Embedding of GAE and TIGAE
$\mathbf{Q}, \mathbf{P} \in \mathbb{R}^{N \times k}$	Soft clustering and target distribution
$\mathbf{Y} \in \mathbb{R}^N$	Clustering labels
$\ \cdot\ _2$	L_2 -norm
\odot	Hadamard product
$\mathcal{S}(\cdot)$	The function of cosine similarity
$CE(\cdot, \cdot)$	Cross entropy loss function
Sigmoid, ReLU	Non-linear activation function
R_h	Homophily rate

indicate the value for the l -th iteration. The complete notations and corresponding explanations are listed in Table I.

B. Transform Input Graph Auto-Encoder (TI)

GAE employs two graph convolutional layers for encoding attributes and structures. It decodes the embeddings by computing inner products, which can be described as follows.

$$\mathbf{H} = \tilde{\mathbf{L}}\text{ReLU}(\tilde{\mathbf{L}}\mathbf{X}\mathbf{W}_1)\mathbf{W}_2, \hat{\mathbf{A}} = \text{Sigmoid}(\mathbf{H}\mathbf{H}^\top). \quad (1)$$

We introduce a linear transformation layer with bias before GAE to build TIGAE to mitigate the above representation collapse issue. This uncomplicated transformation brings two benefits. Firstly, it facilitates dimension reduction, adjusting the feature space for effective information propagation. Secondly, including a bias matrix in the linear transformation process will indirectly incorporate explicit structure information, enhancing cohesion and discriminability. The formal expression of TIGAE is described as

$$\mathbf{Z} = \tilde{\mathbf{L}}\text{ReLU}(\tilde{\mathbf{L}}(\mathbf{X}\mathbf{W}_a^\top + \mathbf{W}_b)\mathbf{W}_1)\mathbf{W}_2, \quad (2)$$

$$\hat{\mathbf{A}}_p = \text{Sigmoid}(\mathbf{Z}\mathbf{Z}^\top).$$

In the following context, \mathbf{X}_p or \mathbf{X}_t will be used to represent $\mathbf{X}\mathbf{W}_a^\top + \mathbf{W}_b$. If the ReLU activation function is not used, the expression for \mathbf{Z} in Eq. (2) can be represented as follows.

$$\mathbf{Z} = \tilde{\mathbf{L}}^2\mathbf{X}\mathbf{W}_a^\top\mathbf{W}_1\mathbf{W}_2 + \tilde{\mathbf{L}}^2\mathbf{W}_b\mathbf{W}_1\mathbf{W}_2. \quad (3)$$

The second term in Eq. (3) is equivalent to $\tilde{\mathbf{L}}(\tilde{\mathbf{L}}\mathbf{W})\mathbf{W}_2$ with $\mathbf{W} = \mathbf{W}_b\mathbf{W}_1$, which can be regarded as the linearly transformed $\tilde{\mathbf{L}}$ propagated on the original graph. As a result, compared with GAE, the encoder of TIGAE incorporates richer information into the final embeddings. This results in more precise reconstructed graphs during decoding. To avoid arbitrarily transforming from the linear layer, we introduce a cross entropy loss between the node similarity of raw attribute

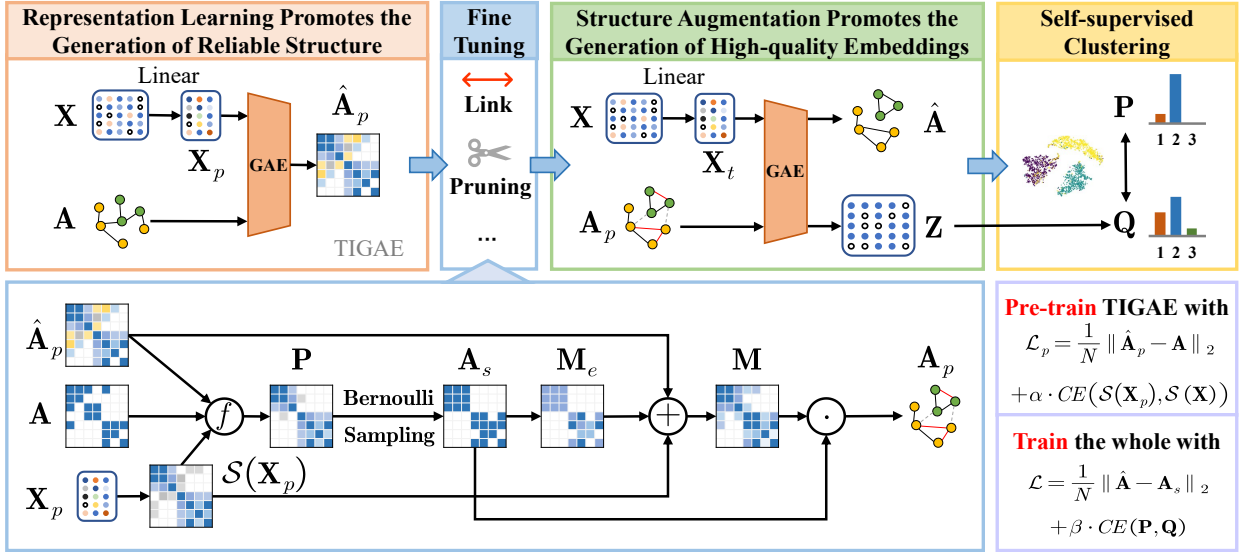


Fig. 2. Illustration of our proposed SynC framework. The TIGAE combines linear transformation with graph convolutional networks. Firstly, we employ the pre-trained TIGAE to generate a predicted graph without a gradient. Secondly, in the fine-tuning phase, we apply the structure fine-tuning strategy to prune, connect, and assign weights to edges in the predicted graph. Subsequently, the refined graph is fed into TIGAE to learn information from neighbor nodes and obtain the final embeddings with a gradient. This is the synergistic interaction of representation learning and structure augmentation since the two TIGAE modules share weights. Finally, we conduct self-supervised clustering in the clustering phase using more cohesive and stronger discriminative embeddings.

\mathbf{X} and that of transformed attribute \mathbf{X}_p . TIGAE is optimized by the following loss function:

$$\mathcal{L}_p = \frac{1}{N} \|\hat{A}_p - \tilde{A}\|_2 + \alpha \cdot CE(\mathcal{S}(\mathbf{X}_p), \mathcal{S}(\mathbf{X})), \quad (4)$$

where α is a trade-off hyper-parameter.

C. Structure Fine-tuning Strategy (T2)

Although we can predict the graph by sampling from the reconstructed graph, obtaining the predicted graph solely from both probabilities and the original graph may still exhibit biases. This is because the probabilities are calculated by embedding, which is obtained by GCN on the unreliable original graph. As a result, a comprehensive structure fine-tuning strategy is proposed to refine the graph by considering multiple factors for better graph representation learning. Specifically, we calculate the cosine similarity of \mathbf{X}_p and average it with the edges prediction probabilities at first:

$$\mathbf{P}' = (\hat{A}_p^{(l)} + \mathcal{S}(\mathbf{X}_p^{(l)}))/2. \quad (5)$$

Compared with $\mathcal{S}(\mathbf{X}^{(l)})$, there are more obvious differences in $\mathcal{S}(\mathbf{X}_p^{(l)})$. Additional edges with the highest probability are added in the graph, which is missing in the original graph:

$$\begin{aligned} \mathbf{P}'_r &= \mathbf{P}' - \mathbf{P}' \odot \tilde{A}, \\ \mathbf{A}_{\text{add}ij}^{(l)} &= \mathbf{A}_{\text{add}ij}^{(l)} = 1 \text{ if } \mathbf{P}'_{rij} == \max(\mathbf{P}'_i) \text{ else } 0, \\ \mathbf{A}_{\text{mask}}^{(l)} &= (\tilde{A} + \mathbf{A}_{\text{add}}^{(l)}). \end{aligned} \quad (6)$$

Next, Bernoulli sampling is introduced to generate an adjacency matrix according to the modified edges probabilities:

$$\begin{aligned} \mathbf{P}^{(l)} &= \mathbf{P}' \odot \mathbf{A}_{\text{mask}}^{(l)}, \\ \mathbf{A}_{sij}^{(l)} &= \text{Bernoulli}(p = \mathbf{P}_{ij}^{(l)}). \end{aligned} \quad (7)$$

It is important to note that the sampled matrix may be asymmetrical, deviating from the prerequisites of an undirected graph. Accounting for this, we assign a default edge weight of 0.5 for the unidirectional edges as a punishment:

$$\mathbf{A}_s^{(l)} = (\mathbf{A}_s^{(l)} + \mathbf{A}_s^{(l)\top})/2. \quad (8)$$

If two nodes with high degrees are connected, the link plays a more crucial role in information propagation. We calculate the importance of each edge according to the degree matrix:

$$\mathbf{M}_e^{(l)} = L_2(\tilde{\mathbf{D}}_s \mathbf{A}_s^{(l)} \tilde{\mathbf{D}}_s), \quad (9)$$

where $\tilde{\mathbf{D}}_s$ is the degree matrix of $\mathbf{A}_s^{(l)}$ and L_2 represents L_2 normalization. Finally, we integrate the edges prediction probabilities, cosine similarities, and importance of edges to derive more accurate confidence of edges. The final graph refined by our structure fine-tuning strategy is calculated by:

$$\begin{aligned} \mathbf{M}^{(l)} &= (\hat{A}_p^{(l)} + \mathcal{S}(\mathbf{X}_p^{(l)}) + \mathbf{M}_e^{(l)})/3, \\ \mathbf{A}_p^{(l)} &= \mathbf{M}^{(l)} \odot \mathbf{A}_s^{(l)}. \end{aligned} \quad (10)$$

D. Synergistic Interaction Architecture (T3)

Performing graph representation learning on the predicted graph generated from neural networks is an exciting attempt. However, the overall model is complicated if the GNN used to predict the graph differs from downstream networks. Moreover, generating a graph before inputting it into downstream networks requires sampling from the probabilities of the predicted edges, involving non-differentiable operations that hinder the backward propagation process.

To address these concerns, we design a novel synergistic interaction architecture of representation learning and structure augmentation to leverage the advantages of TIGAE that TIGAE excels in learning high-quality embeddings and performing graph reconstruction. Specifically, we first pre-train

TIGAE to obtain reliable weights, ensuring a more reliable predicted graph during the first iteration. Then, we conduct forward propagation using these weights without computing gradients to obtain the probabilities of the predicted edges. The process can be described as:

$$\begin{aligned}\mathbf{Z}_p^{(l)} &= \tilde{\mathbf{L}}^{(l)} \text{ReLU}(\tilde{\mathbf{L}}^{(l)} \mathbf{X}_p^{(l)} \mathbf{W}_1^{(l-1)}) \mathbf{W}_2^{(l-1)}, \\ \hat{\mathbf{A}}_p^{(l)} &= \text{Sigmoid}(\mathbf{Z}_p^{(l)} \mathbf{Z}_p^{(l)\top}),\end{aligned}\quad (11)$$

where l represents the l -th iteration, $\mathbf{W}_1^{(0)}$ and $\mathbf{W}_2^{(0)}$ are pre-trained weights. Then, we apply the structure fine-tuning strategy to refine the predicted graph. Subsequently, the augmented graph is used as the input for TIGAE, and forward propagation is executed again with gradient computation at this time so that the TIGAE can be optimized iteratively by using gradient descent. The process is expressed as:

$$\begin{aligned}\mathbf{Z}^{(l)} &= \tilde{\mathbf{L}}_p^{(l)} \text{ReLU}(\tilde{\mathbf{L}}_p^{(l)} \mathbf{X}_t^{(l)} \mathbf{W}_1^{(l)}) \mathbf{W}_2^{(l)}, \\ \hat{\mathbf{A}}^{(l)} &= \text{Sigmoid}(\mathbf{Z}^{(l)} \mathbf{Z}^{(l)\top}),\end{aligned}\quad (12)$$

where $\tilde{\mathbf{L}}_p^{(l)}$ is the symmetric normalized adjacency matrix of the augmented graph $\mathbf{A}_p^{(l)}$. Then, backward propagation based on the loss function is conducted to optimize the weights, which will be discussed in the next section.

We significantly reduced parameter counts by the synergistic interaction of representation learning and structure augmentation implemented by a single TIGAE. We successfully addressed the backward propagation issue caused by sampling. Shared weights enable TIGAE to augment the structure and learn cohesive representations effectively. Compared with two TIGAEs optimized by separate weights, the parameters are theoretically reduced by 50% through sharing weights in our synergistic interaction framework.

E. Self-Supervised Clustering (T4)

The synergistic interaction of representation learning and structure augmentation contributes to the final embeddings, resulting in strong cohesiveness and discrimination. Although employing K-Means directly on the embeddings yields commendable outcomes, we adopt a self-supervised method [14], [22], [42] to achieve better clustering performance. The computation of the soft clustering assignment distribution \mathbf{Q} is as follows:

$$q_{ij} = \frac{(1 + \|\mathbf{z}_i - \boldsymbol{\mu}_j\|^2)^{-1}}{\sum_{j'} (1 + \|\mathbf{z}_i - \boldsymbol{\mu}_{j'}\|^2)^{-1}}, \quad (13)$$

where $\boldsymbol{\mu}_j$ signifies a central vector of the j -th cluster initialized by K-Means on the embeddings of pre-trained TIGAE. The self-supervised target distribution \mathbf{P} is calculated by:

$$p_{ij} = \frac{q_{ij}^2 / \sum_i q_{ij}}{\sum_{j'} q_{ij'}^2 / \sum_i q_{ij'}}. \quad (14)$$

The loss function consisting of reconstruction loss and clustering loss is defined to optimize the framework iteratively:

$$\mathcal{L} = \frac{1}{N} \|\hat{\mathbf{A}} - \mathbf{A}_s\|_2 + \beta \cdot CE(\mathbf{P}, \mathbf{Q}), \quad (15)$$

Algorithm 1: The process of pre-training TIGAE.

Input: Attribute \mathbf{X} ; Structure \mathbf{A} ; Iterations I_m ;
Epoch flag $i = 1$; Hyper-parameter α .

Output: Model's weights.

- 1: **while** $i \leq I_m$ **do**
 - 2: Perform linear transformation on \mathbf{X} ;
 - 3: Obtain \mathbf{Z} and reconstructed $\hat{\mathbf{A}}$ by Eq. (2);
 - 4: Calculate the loss \mathcal{L}_p by Eq. (4);
 - 5: Perform backward propagation;
 - 6: $i = i + 1$;
 - 7: **end while**
 - 8: Save the weights file.
-

where β is a hyper-parameter. For each node, the maximum value of $q_{.j}$ determines the cluster to which it belongs. The clustering label \mathbf{Y} is:

$$y_i = \arg \max_j q_{ij}, \quad j = 1, 2, \dots, k. \quad (16)$$

Algorithm 1 shows the pre-training process of TIGAE and Algorithm 2 shows the complete training process of SynC.

F. Computational Complexity Analysis (T5)

For our proposed TIGAE, the computational complexity introduced by the linear transformation is $\mathcal{O}(Ndc)$, where N is the number of nodes, d is the dimension of the input attributes, and c is the dimension of the linear transformation. Assume that $d = 2c$, then the additional complexity of GAE with twice computations of GCN is $\mathcal{O}(N(N+d_1)c)$ compared with TIGAE, where d_1 is the dimension of the output embeddings after the first graph convolutional transformation. Therefore, when $N + d_1 > d$, the computational complexity of TIGAE is smaller than GAE. As for the fine-tuning strategy, the main complexity comes from Eq. (9). Its complexity even reaches $\mathcal{O}(N^3)$, greatly limiting the model's scalability. In addition, the space complexity of SynC is dominated by the dense adjacency matrix and similarity matrix, resulting in a space complexity of $\mathcal{O}(N^2)$. This is another reason why SynC struggles to scale to large-scale graphs.

IV. EXPERIMENTAL RESULTS AND DISCUSSION

In this section, we validate our proposed SynC through experiments and address the following key questions:

- Q1. Does SynC outperform state-of-the-art methods in clustering performance?
- Q2. Are the TIGAE, structure fine-tuning strategy, and synergistic interaction mechanism in SynC effective?
- Q3. Are the factors considered in the structure fine-tuning strategy effective in improving clustering performance?
- Q4. How does SynC perform on datasets with extremely imbalanced classes and very low homophily ratio?
- Q5. How sensitive is SynC to hyper-parameters?
- Q6. What are the SynC loss function's convergence properties and its clustering accuracy's stability?
- Q7. How cohesive and discriminative are the embeddings learned by SynC?
- Q8. What are the time and space consumption of SynC?

Algorithm 2: The clustering process of SynC.

Input: Attribute \mathbf{X} ; Structure \mathbf{A} ; Iterations I_m ;
 Number of clusters k ; Epoch flag $l = 1$;
 Hyper-parameter β .

Output: Clustering label \mathbf{Y} .

- 1: Pre-train TIGAE with Eq. (4) and initialize SynC;
- 2: **while** $l \leq I_m$ **do**
- 3: Perform gradient-free forward propagation on the TIGAE to predict edge probabilities $\hat{\mathbf{A}}_p^{(l)}$;
- 4: Utilize the fine-tuning strategy to enhance $\mathbf{A}_p^{(l)}$;
- 5: Perform forward propagation on the TIGAE with augmented graph to compute embeddings $\mathbf{Z}^{(l)}$;
- 6: Calculate \mathbf{Q} and \mathbf{P} by Eq. (13) and Eq. (14);
- 7: Calculate total loss \mathcal{L} by Eq. (15);
- 8: Perform backward propagation;
- 9: $l = l + 1$;
- 10: **end while**
- 11: Obtain \mathbf{Y} by Eq. (16).
- 12: **return** \mathbf{Y} .

TABLE II
 STATISTICS OF THE EIGHT DATASETS.

Dataset	#Samples	#Classes	#Dimension	#Edges	R_h
UAT	1190	4	239	13599	0.70
CORA	2708	7	1433	5278	0.81
ACM	3025	3	1870	13128	0.82
CITE	3327	6	3703	4552	0.74
DBLP	4057	4	334	3528	0.80
AMAP	7650	8	745	119081	0.83
Wisconsin	251	5	1703	515	0.20
Texas	183	5	1703	325	0.11

A. Experimental Setup

1) *Datasets:* We conducted extensive experiments on six benchmark datasets to validate the effectiveness of SynC, including ACM, CITE, DBLP, AMAP [9], CORA, and UAT [5]. We also validated our method on the Wisconsin and Texas [43] datasets, known for their low homophily ratio and imbalanced classes. The statistics of datasets are listed in Table II, where R_h represents the homophily ratio [44]. Due to the fact that neither our method nor the comparison methods have been designed with effective large-scale data training methods, we did not utilize large-scale datasets.

2) *Baselines:* We compared SynC with several state-of-the-art methods, including vanilla GAE [8], SDCN [22], DFCN [23], DCRN [9], AGC-DRR [3], CCGC [28], HSAN [5], R²FGC [26]. These methods are detailed in the related work. For the partial experimental results, we directly cited the original papers. We evaluated HSAN and CCGC on the datasets ACM and DBLP, and evaluated GAE and AGC-DRR on the dataset UAT using the open-source codes³. In the comparison experiments, we kept the structure of other models unchanged. We selected the dataset parameters not mentioned in the original paper based on the provided dataset parameters. Specifically, for the AGC-DRR, all parameters remained the same as other datasets on the UAT. The HSAN matched the

TABLE III
 EXPERIMENTAL SETTINGS ON THE EIGHT DATASETS.

Dataset	Pre-training			Training			Transform dimension
	lr	epoch	α	lr	epoch	β	
UAT	2e-3	50	0	1e-3	50	1	128
CORA	2e-3	80	0	5e-3	50	0	128
ACM	1e-3	50	0	2e-3	50	1	512
CITE	2e-3	20	1	6e-3	50	1	512
DBLP	2e-3	20	1	2e-2	50	1	512
AMAP	1e-3	80	1	1e-4	50	1	512
Wisconsin	1e-2	20	1	1e-2	50	1	512
Texas	5e-3	20	10	5e-3	50	0	512

CORA dataset parameters on the ACM dataset, while no PCA dimensionality reduction was performed on the DBLP. The CCGC had a learning rate of 1e-3 on the DBLP and 1e-4 on the ACM, with 400 iterations, as mentioned in the paper. The GAE used a learning rate 1e-3 and 50 epochs on the UAT.

3) *Metrics:* We evaluated our approach using four commonly used metrics for graph clustering, which are also used in the papers of comparative methods [9], [22]: accuracy (ACC), normalized mutual information (NMI), adjusted rand index (ARI), and macro F1-score (F1). The higher the value, the better performance. In addition, we used Welch’s t-test [45] to perform a significance test at the 0.05 significance level. The metrics are calculated as follows:

4) *Training Procedure and Parameters Settings:* Table III lists the detailed information on the specific learning rates and hyper-parameter settings. To ensure the reliability of clustering and initial cluster centers during the training phase, we conducted pre-training on TIGAE. Specifically, except for UAT and CORA, where the linear transformation dimension was set to 128, the other datasets had a linear transformation dimension 512. The hyper-parameter α was set to 0 on the ACM, CORA, and UAT. Each dataset was pre-trained iteratively for a minimum of 20 epochs. We first loaded the pre-trained parameters in the training phase and then trained them with 50 epochs for optimal convergence. Most experiments were conducted on a Tesla T4 GPU (16G) and were programmed with PyTorch 2.1.0; time and space consumption experiments were conducted on an NVIDIA GTX 1050 GPU (2G) and an Intel(R) Core(TM) i5-8300H CPU 2.30GHz. We conducted ten experiments and reported the mean and standard deviation (mean \pm std) to mitigate system errors. For the reproducibility of experiments, the random seed was set to 325 for pre-training and training.

B. Comparative analysis (Q1)

Table IV shows the clustering results regarding various baselines and metrics. We make the following key insights:

- 1) Compared with the classical deep clustering approaches, our method enhances the quality of the input data from both attribute and structure perspectives, thus fully leveraging the powerful aggregation capabilities of GCNs. Notably, using the same GAE base architecture, our method achieves a significant improvement in accuracy by 22% and ARI by 39.67% on the dataset DBLP compared with GAE. Furthermore, compared with the state-of-the-art methods, our approach exhibits a remarkable

³A-Unified-Framework-for-Deep-Attribute-Graph-Clustering

TABLE IV

CLUSTERING RESULTS ON SIX DATASETS. THE BEST IS HIGHLIGHTED IN BOLD, AND THE ASTERISK (*) DENOTES THE SECOND BEST. $\uparrow, \downarrow, \sim$ RESPECTIVELY INDICATE SIGNIFICANT IMPROVEMENT, SIGNIFICANT DECREASE, AND NO SIGNIFICANT CHANGE AT THE 0.05 SIGNIFICANCE LEVEL.

Datasets	Metrics	Vanilla GAE NeurIPS'16	SDCN WWW'20	DFCN AAAI'21	DCRN AAAI'22	AGC-DRR IJCAI'22	CCGC AAAI'23	HSAN AAAI'23	R ² FGC TNNLS'23	SynC KMeans	SynC SSL	p-value
ACM	ACC	84.52±1.44	90.45±0.18	90.90±0.20	91.93±0.20	92.55±0.09*	88.76±0.91	82.50±2.47	92.43±0.18	91.51±0.12	92.73±0.04	0.00†
	NMI	55.38±1.92	68.31±0.25	69.40±0.40	71.56±0.61	72.89±0.24*	64.28±1.88	52.22±4.45	72.42±0.53	70.01±0.26	73.58±0.22	0.00†
	ARI	59.46±3.10	73.91±0.40	74.90±0.40	77.56±0.52	79.08±0.24*	69.86±2.09	55.12±5.58	78.72±0.47	76.43±0.30	79.58±0.11	0.00†
	F1	84.65±1.33	90.42±0.19	90.80±0.20	91.94±0.20	92.55±0.09*	88.71±0.91	82.43±2.51	92.45±0.18	91.49±0.12	92.74±0.04	0.00†
DBLP	ACC	61.21±1.22	68.05±1.81	76.00±0.80	79.66±0.25	80.41±0.47	65.19±4.20	71.91±0.96	80.95±0.20*	77.62±0.55	83.48±0.13	0.00†
	NMI	30.80±0.91	39.50±1.34	43.70±1.00	48.95±0.44	49.77±0.65	33.48±3.94	42.74±0.63	50.82±0.32*	45.62±1.54	55.11±0.24	0.00†
	ARI	22.02±1.40	39.15±2.01	47.00±1.50	53.60±0.46	55.39±0.88	34.21±5.43	43.81±1.29	56.34±0.42*	50.17±1.18	61.70±0.27	0.00†
	F1	61.41±2.23	67.71±1.51	75.70±0.80	79.28±0.26	79.90±0.45	64.00±4.29	71.13±1.23	80.54±0.19*	77.19±0.54	82.90±0.17	0.00†
CITE	ACC	61.35±0.80	65.96±0.31	69.50±0.20	70.86±0.18	68.32±1.83	69.84±0.94	71.15±0.80*	70.60±0.45	66.93±0.80	71.77±0.27	0.04†
	NMI	34.63±0.65	38.71±0.32	43.90±0.20	45.86±0.35*	43.28±1.41	44.33±0.79	45.06±0.74	45.39±0.37	40.49±0.53	46.37±0.42	0.01†
	ARI	33.55±1.18	40.17±0.43	45.50±0.30	47.64±0.30*	45.34±2.33	45.68±1.80	47.05±1.12	47.07±0.30	41.52±0.88	48.09±0.45	0.02†
	F1	57.36±0.82	63.62±0.24	64.30±0.20	65.83±0.21	64.82±1.60	62.71±2.06	63.01±1.79	65.28±0.12	62.97±0.36	65.72±0.36*	0.42~
CORA	ACC	68.09±2.59	35.60±2.83	36.33±0.49	61.93±0.47	40.62±0.55	73.88±1.20	77.07±1.56	-	77.22±0.40*	78.58±0.38	0.00†
	NMI	47.77±2.53	14.28±1.91	19.36±0.87	45.13±1.57	18.74±0.73	56.45±1.04	59.21±1.03	-	57.26±0.57	58.13±0.52*	0.01↓
	ARI	42.52±3.10	0.78±3.24	0.47±2.10	33.15±0.14	14.80±1.64	52.51±1.89	57.52±2.70*	-	55.34±0.64	57.90±1.06	0.69~
	F1	67.11±2.71	24.37±1.04	26.16±0.50	49.50±0.42	31.23±0.57	70.98±2.79	75.11±1.40	-	76.31±0.41*	77.65±0.30	0.00†
AMAP	ACC	71.57±2.48	53.44±0.81	76.88±0.80	79.94±0.13	78.11±1.69	77.25±0.41	77.02±0.33	81.28±0.05*	80.94±0.11	82.48±0.10	0.00†
	NMI	62.13±2.79	44.85±0.83	69.21±1.00	73.70±0.24*	72.21±1.63	67.44±0.48	67.21±0.33	73.88±0.17	68.92±0.18	69.70±0.23	0.00↓
	ARI	48.82±4.57	31.21±1.23	58.98±0.84	63.69±0.20	61.15±1.65	57.99±0.66	58.01±0.48	66.25±0.36	61.85±0.54	65.02±0.11*	0.00↓
	F1	68.08±1.76	50.66±1.49	71.58±0.31	73.82±0.12	72.72±0.97	72.18±0.57	72.03±0.46	75.29±0.32	79.51±0.40*	80.69±0.11	0.00†
UAT	ACC	55.18±0.46	52.25±1.91	33.61±0.09	49.92±1.25	52.57±1.44	56.34±1.11	56.04±0.67	-	60.39±0.46	57.33±0.13*	0.00†
	NMI	23.40±0.96	21.61±1.26	26.49±0.41	24.09±0.53	23.75±1.47	28.15±1.92	26.99±2.11	-	30.26±0.62	28.58±0.24*	0.00†
	ARI	22.44±1.34	21.63±1.49	11.87±0.23	17.17±0.69	21.73±0.85	25.52±2.09	25.22±1.96	-	30.09±0.76	26.60±0.17*	0.00†
	F1	54.39±0.89	45.59±3.54	25.79±0.29	44.81±0.87	51.97±2.10	55.24±1.69	54.20±1.84	-	58.91±1.02	57.34±0.23*	0.00†

improvement of 4.27% in NMI and 5.35% in ARI on the dataset DBLP.

- SynC still achieves competitive results on many datasets even when using K-Means, especially on the small-scale UAT data, demonstrating that our proposed embedding representation learning method is effective.
- Methods (e.g., AGC-DRR, R²FGC) that employ specific attribute or structure learning and optimization strategies tend to outperform those that neglect such considerations, which is because GCN is unable to detect and process anomalous information during the learning process effectively, and unprocessed data may impede the propagation of meaningful information, thereby compromising the discriminability of the learned embeddings.
- While contrastive learning-based methods (e.g., CCGC, HSAN) have shown favorable clustering results, the significant variations of standard deviation indicate that they may lack stability, making it impossible to apply them practically without supervision.
- We also note that the performance of our SynC on NMI and ARI improves slightly on the class-imbalanced datasets (e.g., AMAP) because the embeddings' discriminability of different clusters learned by our method is not very distinguishable on these datasets.

In conclusion, the significant improvements demonstrate that our proposed method exhibits excellent clustering performance on common benchmark datasets.

C. Ablation Study (Q2-Q4)

1) *Modules Analysis (Q2)*: We designed three variants and conducted ablation experiments to validate the effectiveness of different modules in our method. The details of different variants are listed as follows, and the results are depicted in Fig. 3.

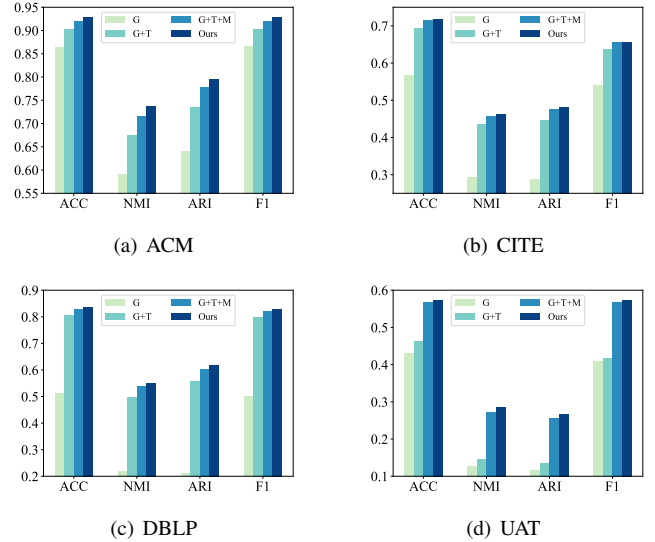


Fig. 3. Ablation results of the proposed SynC on four datasets.

- “G”: This variant is vanilla GAE, which is used to be compared as a basic model.
- “G+T”: This variant is our proposed TIGAE. Comparing it with “G”, we can get the performance of TIGAE in solving the representation collapse issue of GAE.
- “G+T+M”: This variant is our proposed synergistic interaction framework based on TIGAE. Comparing it with “G+T”, we can validate the advantages of synergistic interaction of representation learning and structure augmentation. Comparing it with SynC reveals the effect of the structure fine-tuning strategy.

As shown in Fig. 3, every module in our method can improve clustering performance. Specifically, compared with “G”, “G+T” performs better because TIGAE incorporates explicit structure information. Moreover, comparing “G+T”

with ‘‘G+T+M’’, we conclude that the synergistic interaction framework using TIGAE improves the performance, especially on the dataset UAT. While the structure fine-tuning does not significantly improve clustering performance on the datasets with high homophily ratio by comparing our method with ‘‘G+T+M’’, it prevents the predicted graph from deviating from the original graph. The synergistic deep graph clustering network based on TIGAE can effectively improve clustering performance.

TABLE V
CLUSTERING RESULTS WITH DIFFERENT STRUCTURE FINE-TUNING FACTORS.

Weighting			✓
Link			✓
Pruning	✓	✓	✓
ACM	91.99±0.06	92.55±0.13	92.73±0.05
DBLP	82.86±0.09	83.30±0.26	83.47±0.15
CORA	77.77±0.44	78.09±0.47	78.58±0.38
Wisconsin	55.34±1.25	58.13±0.88	59.64±1.02
Texas	60.49±1.34	62.73±1.06	64.37±0.80

2) *Structure Fine-tuning Strategy Analysis (Q3, Q4)*: Although the Structure Fine-tuning (SF) strategy has higher complexity and brings only marginal benefits on graphs with a high homophily ratio, its effectiveness is significantly enhanced on datasets with a low homophily ratio and imbalanced classes. Table V presents the results of ablation experiments on different factors within SF, demonstrating that ‘Pruning’, ‘Link’, and ‘Weighting’ are all effective strategies. Notably, ‘Link’ shows the most significant improvement in clustering results in Wisconsin and Texas.

TABLE VI
COMPARISON OF CLUSTERING RESULTS FROM DIFFERENT METHODS ON THE WISCONSIN DATASET.

Methods	Metrics			
	ACC	NMI	ARI	F1
SDCN	50.48±1.72	9.47±2.80	8.56±3.83	23.23±3.49
DFCN	50.72±0.56	11.48±0.48	12.92±0.56	25.26±0.90
DCRN	51.20±0.32	8.89±0.57	7.89±0.69	23.88±0.47
HSAN	47.97±0.41	10.31±0.78	12.04±0.69	28.84±0.62
w/o SF	54.06±1.32*	24.61±2.87*	19.01±1.98*	33.39±1.96*
SynC	59.64±1.02	32.79±1.42	26.86±1.30	38.19±1.30
p-value	0.00↑	0.00↑	0.00↑	0.00↑

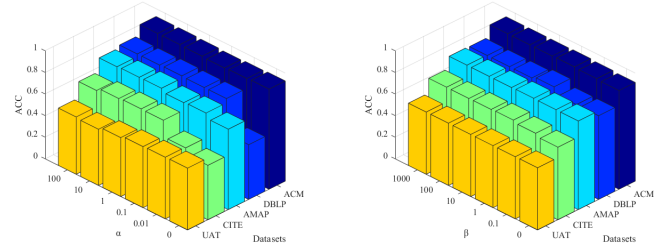
TABLE VII
COMPARISON OF CLUSTERING RESULTS FROM DIFFERENT METHODS ON THE TEXAS DATASET.

Methods	Metrics			
	ACC	NMI	ARI	F1
SDCN	59.40±1.71	12.10±3.30	14.19±5.66	26.60±3.85
DFCN	60.60±0.79	14.57±0.62	26.71±1.47*	30.71±1.03
DCRN	61.26±0.45	16.00±2.02	17.87±2.72	29.06±1.92
HSAN	59.78±0.36	14.64±0.36	24.45±0.48	35.29±1.50*
w/o SF	59.02±1.42*	21.53±1.66*	22.97±2.14	34.19±2.46
SynC	64.37±0.80	27.61±1.00	32.65±1.91	39.49±1.53
p-value	0.00↑	0.00↑	0.00↑	0.00↑

We further compared our method with several state-of-the-art approaches on the Wisconsin and Texas datasets. The results are presented in Tables VI and VII. It can be observed that our method significantly improves clustering performance, mainly due to the SF strategy. Moreover, our method achieved

competitive results comparable to the baselines even without using the SF strategy (w/o SF).

D. Hyper-parameter Analysis (Q5)



(a) Pre-training with different α .

(b) Training with different β .

Fig. 4. Clustering results with different hyper-parameters.

Regarding the hyper-parameter α in Eq. (4), we conducted sensitivity experiments by selecting α from $\{0, 0.01, 0.1, 1, 10, 100\}$ and selecting β from $\{0, 0.1, 1, 10, 100, 1000\}$. As shown in Fig. 4(a), α does not significantly impact the results for ACM, AMAP, and UAT. The function of α is to control how much the original data similarity is preserved during the linear transformation. Therefore, the tiny similarity differentiation makes α less meaningful for these datasets. However, for the other datasets, feature similarity of raw data provides crucial information for preventing arbitrary linear transformation. Fortunately, α is insensitive to values other than 0 for these datasets. Fig. 4(b) shows that our method is insensitive to β , which is usually set to 1. Nevertheless, optimizing using the cross-entropy loss between the auxiliary distribution \mathbf{P} and the clustering distribution \mathbf{Q} is not always effective. For example, the best results are achieved on the CORA and Texas datasets when β is set to 0. Even so, we still believe that SynC is not sensitive to the value of β . Consequently, SynC is only sensitive to whether to set α to 0 when the feature similarity is informative.

E. Convergence Analysis (Q6)

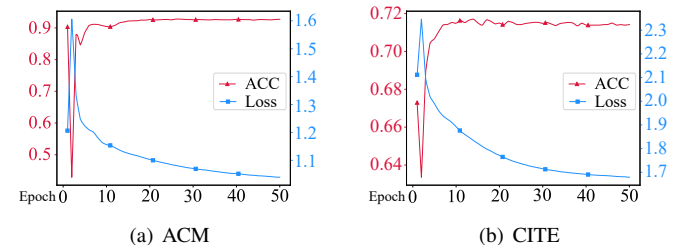


Fig. 5. Convergence effect on different datasets.

To demonstrate the rapid convergence of our method, we conducted experiments on two datasets. We tracked the variations in loss and accuracy throughout the iterations, which are depicted in Fig. 5. Our approach consistently converged on all datasets, reaching optimal performance within around 20 epochs. During the second iteration, we observed a sharp

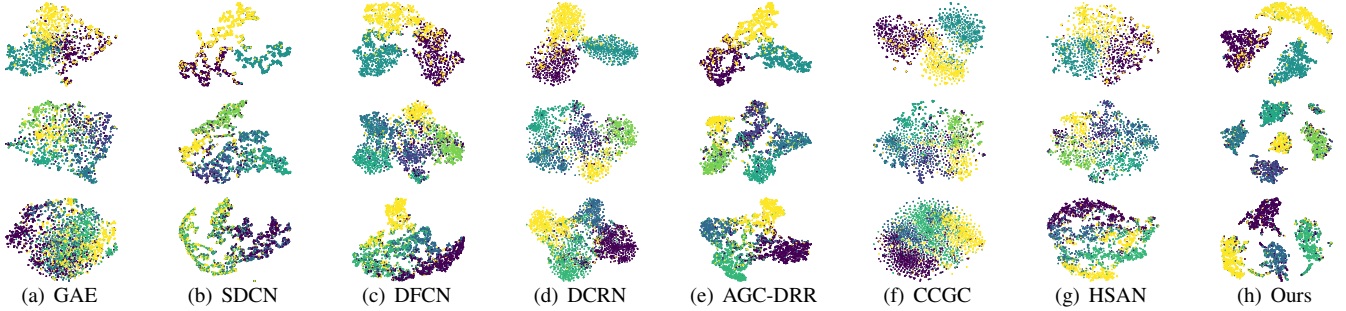


Fig. 6. 2D t -SNE visualization of eight methods. From the first row to the third row, the datasets are ACM, CITE, DBLP.

increase in the loss value and a decline in the accuracy. It can be primarily caused by the loss used in pre-training, which differs from training, so using pre-trained parameters has a lower loss in the initial stage. However, as we modified the graph and re-aggregated the features, the discriminative ability of the embeddings was compromised, leading to a sharp increase in clustering loss. This phenomenon gradually disappears as the synergistic interaction of representation learning and structure augmentation works. Therefore, our method demonstrates excellent convergence.

F. Visualization Analysis (Q7)

t -SNE [42] visualization on the final embeddings was conducted to provide visual evidence of the superior performance of SynC. As depicted in Fig. 6, SynC outperforms the current state-of-the-art methods, exhibiting superior cluster distribution regarding cohesion and discriminability attributed to the synergistic interaction of representation learning and structure augmentation.

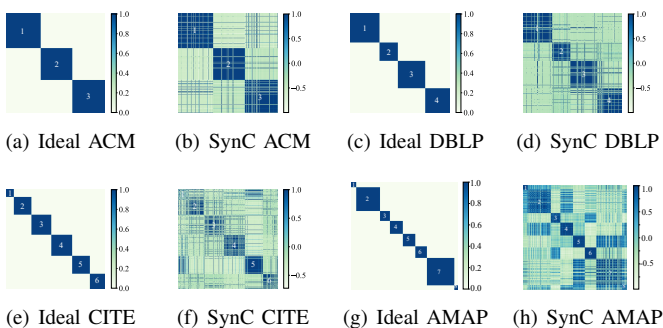


Fig. 7. Ideal embeddings and SynC embeddings similarity heat maps.

Similarity heat maps of embeddings were also drawn to visualize the high-quality embeddings learned by our method, which have both strong cohesion and discriminability. As shown in Fig. 7, our method performs well in identifying significant clusters and learning cluster-consistent features. At the same time, the features acquired from distinct clusters using our approach exhibit a nearly total dissimilarity. Nevertheless, there are still some challenging nodes that are incorrectly categorized.

TABLE VIII
COMPARISON OF TIME AND SPACE CONSUMPTION ON THE ACM.

Methods	SDCN	DCRN	AGC-DRR	HSAN	SynC
Pre-training Time (s)	6.38	38.94	0	0	2.7*
Training Time (s)	14.71*	147.10	2165.31	OOM	11.47
Iterations	50	400*	400*	400*	50
Training Speed (it/s)	3.40*	2.72	0.18	OOM	4.36
Params (M)	6.62	0.60	1.60	10.58	1.09*
Max GPU Memory (MB)	507.71*	1189.40	348.08	1935.58	628.12
Average Rank	2.67*	3.17	2.67*	4	1.67

G. Time and Space Consumption Analysis (Q8)

Performance experiments were conducted to compare the comprehensive performance of SynC with other state-of-the-art methods on the ACM dataset. The evaluation considered various performance indicators, including pre-training time, training time, iterations, training speed (iterations per second), parameter count (Params, in millions), maximum GPU memory (in MB), and average rank. “OOM” denotes “out of memory” when training on a GTX 1050. The results in Table VIII demonstrate that our method achieves the best overall performance.

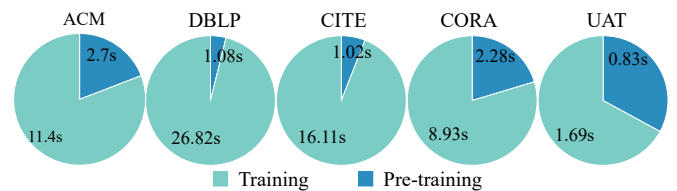


Fig. 8. Pre-training and training time.

Our proposed method requires pre-training first and then fine-tuning. However, experiments on the five datasets in Fig. 8 show that our method does not require too much time in pre-training and fine-tuning, and pre-training only accounts for a small part of the total time. As a result, SynC is the best choice for clustering the small-scale dataset.

V. CONCLUSION AND OUTLOOK

In this paper, we design a Transform Input Graph Auto-Encoder (TIGAE), which utilizes a linear transformation to indirectly incorporate explicit structural information, migrating the representation collapse issue of GAE. Based on the TIGAE, we propose a clustering framework termed Synergistic

Deep Graph Clustering Network (SynC), which fully leverages the feature-smoothing capability of GNNs. TIGAE optimizes the computational complexity of GAE under certain conditions, resulting in faster computational speed for SynC. The structure fine-tuning strategy improve the generalization of SynC. Our method stands out for its state-of-the-art clustering results, fast execution speed, and high stability. Extensive experiments provide accurate and compelling evidence for the outstanding performance of SynC.

Given that the fine-tuning strategy incurs additional computational overhead for marginal performance gains, and it is hard to train on large-scale graphs with mini-batch data, we will focus on developing more efficient fine-tuning strategies in future work.

VI. ACKNOWLEDGMENTS

We sincerely thank the reviewers for taking the time to review this paper and for their valuable suggestions. We also appreciate the constructive suggestions provided by Wei Du and Yue Liu (homepage: <http://yueliu1999.github.io/>).

REFERENCES

- [1] C. Wang, S. Pan, R. Hu, G. Long, J. Jiang, and C. Zhang, "Attributed graph clustering: A deep attentional embedding approach," in *Proc. of IJCAI*. Macao, China: ijcai.org, 2019, pp. 3670–3676.
- [2] Z. Peng, H. Liu, Y. Jia, and J. Hou, "Attention-driven graph clustering network," in *Proc. of ACM MM*. Virtual Event, China: ACM, 2021, pp. 935–943.
- [3] L. Gong, S. Zhou, W. Tu, and X. Liu, "Attributed graph clustering with dual redundancy reduction," in *Proc. of IJCAI*. Vienna, Austria: ijcai.org, 2022, pp. 3015–3021.
- [4] J. Hao and W. Zhu, "Deep graph clustering with enhanced feature representations for community detection," *Applied Intelligence*, vol. 53, no. 2, pp. 1336–1349, 2023.
- [5] Y. Liu, X. Yang, S. Zhou, X. Liu, Z. Wang, K. Liang, W. Tu, L. Li, J. Duan, and C. Chen, "Hard sample aware network for contrastive deep graph clustering," in *Proc. of AAAI*. Washington, DC, USA: AAAI Press, 2023, pp. 8914–8922.
- [6] S. Ding, B. Wu, X. Xu, L. Guo, and L. Ding, "Graph clustering network with structure embedding enhanced," *Pattern Recognit.*, vol. 144, p. 109833, 2023.
- [7] T. N. Kipf and M. Welling, "Semi-supervised classification with graph convolutional networks," 2016.
- [8] —, "Variational graph auto-encoders," *CoRR*, vol. abs/1611.07308, 2016.
- [9] Y. Liu, W. Tu, S. Zhou, X. Liu, L. Song, X. Yang, and E. Zhu, "Deep graph clustering via dual correlation reduction," in *Proc. of AAAI*. Virtual Event: AAAI Press, 2022, pp. 7603–7611.
- [10] Q. Li, Z. Han, and X. Wu, "Deeper insights into graph convolutional networks for semi-supervised learning," in *Proc. of AAAI*. New Orleans, Louisiana, USA: AAAI Press, 2018, pp. 3538–3545.
- [11] T. Zhao, Y. Liu, L. Neves, O. J. Woodford, M. Jiang, and N. Shah, "Data augmentation for graph neural networks," in *Proc. of AAAI*. Virtual Event: AAAI Press, 2021, pp. 11 015–11 023.
- [12] C. J. Maddison, A. Mnih, and Y. W. Teh, "The concrete distribution: A continuous relaxation of discrete random variables," in *International Conference on Learning Representations*, 2017. [Online]. Available: <https://openreview.net/forum?id=S1jE5L5gl>
- [13] J. Hartigan and M. Wong, "Algorithm as 136: A k-means clustering algorithm," *Journal of the royal statistical society. series c (applied statistics)*, vol. 28, no. 1, pp. 100–108, 1979.
- [14] J. Xie, R. B. Girshick, and A. Farhadi, "Unsupervised deep embedding for clustering analysis," in *Proc. of ICML*, ser. JMLR Workshop and Conference Proceedings, vol. 48. New York, NY: JMLR.org, 2016, pp. 478–487.
- [15] X. Guo, L. Gao, X. Liu, and J. Yin, "Improved deep embedded clustering with local structure preservation," in *Proc. of IJCAI*. Melbourne, Australia: ijcai.org, 2017, pp. 1753–1759.
- [16] P. Velickovic, G. Cucurull, A. Casanova, A. Romero, P. Liò, and Y. Bengio, "Graph attention networks," in *Proc. of ICLR*. Vancouver, BC, Canada: OpenReview.net, 2018.
- [17] S. Pan, R. Hu, G. Long, J. Jiang, L. Yao, and C. Zhang, "Adversarially regularized graph autoencoder for graph embedding," in *Proc. of IJCAI*. Stockholm, Sweden: ijcai.org, 2018, pp. 2609–2615.
- [18] C. Wang, S. Pan, G. Long, X. Zhu, and J. Jiang, "MGAE: marginalized graph autoencoder for graph clustering," in *Proc. of CIKM*. Singapore: ACM, 2017, pp. 889–898.
- [19] N. Mrabah, M. Bouguessa, M. F. Touati, and R. Ksantini, "Rethinking graph auto-encoder models for attributed graph clustering," *IEEE Transactions on Knowledge and Data Engineering*, vol. 35, no. 9, pp. 9037–9053, 2023.
- [20] J. Li, R. Wu, W. Sun, L. Chen, S. Tian, L. Zhu, C. Meng, Z. Zheng, and W. Wang, "What's behind the mask: Understanding masked graph modeling for graph autoencoders," in *Proc. of KDD*, ser. KDD '23. New York, NY, USA: Association for Computing Machinery, 2023, p. 1268–1279.
- [21] Z. Hou, Y. He, Y. Cen, X. Liu, Y. Dong, E. Kharlamov, and J. Tang, "Graphmae2: A decoding-enhanced masked self-supervised graph learner," in *Proc. of WWW*, ser. WWW '23. New York, NY, USA: Association for Computing Machinery, 2023, p. 737–746.
- [22] D. Bo, X. Wang, C. Shi, M. Zhu, E. Lu, and P. Cui, "Structural deep clustering network," in *Proc. of WWW*. Taipei, Taiwan: ACM / IW3C2, 2020, pp. 1400–1410.
- [23] W. Tu, S. Zhou, X. Liu, X. Guo, Z. Cai, E. Zhu, and J. Cheng, "Deep fusion clustering network," in *Proc. of AAAI*. Virtual Event: AAAI Press, 2021, pp. 9978–9987.
- [24] G. Huo, Y. Zhang, J. Gao, B. Wang, Y. Hu, and B. Yin, "Caecn: Cross-attention fusion based enhanced graph convolutional network for clustering," *IEEE Transactions on Knowledge and Data Engineering*, vol. 35, no. 4, pp. 3471–3483, 2021.
- [25] X. Zhang, H. Liu, Q. Li, X.-M. Wu, and X. Zhang, "Adaptive graph convolution methods for attributed graph clustering," *IEEE Transactions on Knowledge and Data Engineering*, vol. 35, no. 12, pp. 12 384–12 399, 2023.
- [26] S. Yi, W. Ju, Y. Qin, X. Luo, L. Liu, Y. Zhou, and M. Zhang, "Redundancy-free self-supervised relational learning for graph clustering," *IEEE Transactions on Neural Networks and Learning Systems*, 2023.
- [27] H. Zhao, X. Yang, Z. Wang, E. Yang, and C. Deng, "Graph debiased contrastive learning with joint representation clustering," in *Proc. of IJCAI*. Montreal, Canada: ijcai.org, 2021, pp. 3434–3440.
- [28] X. Yang, Y. Liu, S. Zhou, S. Wang, W. Tu, Q. Zheng, X. Liu, L. Fang, and E. Zhu, "Cluster-guided contrastive graph clustering network," in *Proc. of AAAI*. Washington, DC, USA: AAAI Press, 2023, pp. 10 834–10 842.
- [29] Y. Liu, X. Yang, S. Zhou, X. Liu, S. Wang, K. Liang, W. Tu, and L. Li, "Simple contrastive graph clustering," *IEEE Transactions on Neural Networks and Learning Systems*, pp. 1–12, 2023.
- [30] K. Zhan, C. Zhang, J. Guan, and J. Wang, "Graph learning for multiview clustering," *IEEE Transactions on Cybernetics*, vol. 48, no. 10, pp. 2887–2895, 2018.
- [31] C. Liu, Z. Liao, Y. Ma, and K. Zhan, "Stationary diffusion state neural estimation for multiview clustering," in *Proc. of AAAI*. Virtual Event: AAAI Press, 2022, pp. 7542–7549.
- [32] Z. Liao, X. Zhang, W. Su, and K. Zhan, "View-consistent heterogeneous network on graphs with few labeled nodes," *IEEE Trans. Cybern.*, vol. 53, no. 9, pp. 5523–5532, 2023.
- [33] Y. Liu, K. Liang, J. Xia, S. Zhou, X. Yang, X. Liu, and S. Z. Li, "Dink-net: Neural clustering on large graphs," in *Proc. of ICML*, ser. Proceedings of Machine Learning Research, vol. 202. Honolulu, Hawaii, USA: PMLR, 2023, pp. 21 794–21 812.
- [34] Y. Liu, K. Liang, J. Xia, X. Yang, S. Zhou, M. Liu, X. Liu, and S. Z. Li, "Reinforcement graph clustering with unknown cluster number," in *Proc. of ACM MM*, ser. MM '23. New York, NY, USA: Association for Computing Machinery, 2023, p. 3528–3537.
- [35] Y. Liu, J. Xia, S. Zhou, X. Yang, K. Liang, C. Fan, Y. Zhuang, S. Z. Li, X. Liu, and K. He, "A survey of deep graph clustering: Taxonomy, challenge, application, and open resource," 2023.
- [36] S. Yu, H. Huang, M. N. Dao, and F. Xia, "Graph augmentation learning," in *Proc. of WWW*. Lyon, France: ACM, 2022, pp. 1063–1072.
- [37] P. A. Papp, K. Martinkus, L. Faber, and R. Wattenhofer, "Dropgmn: Random dropouts increase the expressiveness of graph neural networks," in *Proc. of NeurIPS*. virtual: MIT Press, 2021, pp. 21 997–22 009.

- [38] Y. Rong, W. Huang, T. Xu, and J. Huang, "Dropege: Towards deep graph convolutional networks on node classification," in *Proc. of ICLR*. Addis Ababa, Ethiopia: OpenReview.net, 2020.
- [39] Z. Peng, H. Liu, Y. Jia, and J. Hou, "Graph augmentation clustering network," 2022.
- [40] Q. Sun, J. Li, H. Yuan, X. Fu, H. Peng, C. Ji, Q. Li, and P. S. Yu, "Position-aware structure learning for graph topology-imbalance by relieving under-reaching and over-squashing," in *Proc. of CIKM*. Atlanta, GA, USA: ACM, 2022, pp. 1848–1857.
- [41] L. Gong, W. Tu, S. Zhou, L. Zhao, Z. Liu, and X. Liu, "Deep fusion clustering network with reliable structure preservation," *IEEE Transactions on Neural Networks and Learning Systems*, pp. 1–12, 2022.
- [42] L. Van der Maaten and G. Hinton, "Visualizing data using t-sne," *Journal of Machine Learning Research*, vol. 9, no. 11, pp. 2579–2605, 2008.
- [43] H. Pei, B. Wei, K. C.-C. Chang, Y. Lei, and B. Yang, "Geom-gcn: Geometric graph convolutional networks," in *International Conference on Learning Representations*, 2020.
- [44] J. Zhu, Y. Yan, L. Zhao, M. Heimann, L. Akoglu, and D. Koutra, "Beyond homophily in graph neural networks: Current limitations and effective designs," *Advances in neural information processing systems*, vol. 33, pp. 7793–7804, 2020.
- [45] B. L. Welch, "The generalization of 'student's' problem when several different population variances are involved," *Biometrika*, vol. 34, no. 1-2, pp. 28–35, 1947.



Bneyu Wu received his B.Sc. degree from China University of Mining and Technology in 2022. He is currently pursuing the M.Sc. degree in China University of Mining and Technology. His research interests include graph machine learning and clustering analysis.



Lili Guo (Member, IEEE) received her Ph.D. degree from Tianjin University, Tianjin China in 2021. She is a lecturer at China University of Mining and Technology. Her research interests include deep learning, multimodal emotional computing, et al.



Ling Ding received her B.S. degree and M.S. degree from Asia Pacific University of Technology and Innovation, Kuala Lumpur, Malaysia in 2017 and 2019 respectively. She is currently pursuing Ph.D degree in Tianjin University. Her research interests include deep learning, graph machine learning, clustering, et al.



Shifei Ding (Senior Member, IEEE) received Ph.D. degree from Shandong University of Science and Technology, Qingdao, China in 2004, and received post Ph.D. degree from Institute of Computing Technology, and Chinese Academy of Sciences, Beijing, China in 2006, and the head of Joint Laboratory of Intelligent Information Processing, China University of Mining and Technology and Chinese Academy of Sciences. He is a senior member of the IEEE and the IEEE Computer Society, the director and outstanding member of China Computer Federation (CCF), the director and senior member of Chinese Association for Artificial Intelligence (CAAI). His research interests include intelligent information processing, pattern recognition, machine learning, data mining, and granular computing et al.



Xindong Wu (Fellow, IEEE) received the Ph.D. degree from the University of Edinburgh, Edinburgh, U.K. He is a Yangtze River Scholar with the Hefei University of Technology, Hefei, China. His current research interests include data mining, big data analytics, and knowledge engineering. Dr. Wu was the Editor-in-Chief of IEEE Transactions on Knowledge and Data Engineering (TKDE) (2005-2008), and is the Steering Committee Chair of the IEEE International Conference on Data Mining and the Editor-in-Chief of Knowledge and Information Systems. He is a Fellow of the American Association for the Advancement of Science and IEEE.



Xiao Xu received her Ph.D. degree from China University of Mining and Technology, Xuzhou in 2021. She is a lecturer at China University of Mining and Technology. Her research interests include deep learning, clustering analysis, et al.